

Multi-Time-Scale Rolling Optimal Dispatch for Grid-Connected AC/DC Hybrid Microgrids

Authors:

Zhao Luo, Zhendong Zhu, Zhiyuan Zhang, Jinghui Qin, Hao Wang, Zeyong Gao, Zhichao Yang

Date Submitted: 2020-01-20

Keywords: energy management, rolling optimization, multi-time-scale, AC/DC hybrid, microgrids

Abstract:

In order to reduce the impact of the randomness and volatility of renewable energy on the economic operation of AC/DC hybrid microgrids, a multi-time-scale rolling optimization strategy is proposed for the grid-connected AC/DC hybrid microgrids. It considers the source-load uncertainty declined with time scale reduction, and the scheduling cooperation problem of different units on different time scales. In this paper, we propose a three-time-scale optimal strategy of the day-ahead, intraday and real-time dispatching stage and a two-level rolling optimal strategy of the intraday and real-time stage, aiming at minimizing the operating cost. We added the power penalty cost in the rolling optimization model to limit the energy state of the energy storage system in the constraint, and improve the power correction and tracking effect of the rolling optimization. A typical-structure AC/DC hybrid microgrid is analyzed in this paper and the simulation results are shown to demonstrate the feasibility and effectiveness of the proposed multi-time-scale rolling optimal dispatch.

Record Type: Published Article

Submitted To: LAPSE (Living Archive for Process Systems Engineering)

Citation (overall record, always the latest version):

LAPSE:2020.0102

Citation (this specific file, latest version):

LAPSE:2020.0102-1

Citation (this specific file, this version):


LAPSE:2020.0102-1v1

DOI of Published Version: <https://doi.org/10.3390/pr7120961>

License: Creative Commons Attribution 4.0 International (CC BY 4.0)

Article

Multi-Time-Scale Rolling Optimal Dispatch for Grid-Connected AC/DC Hybrid Microgrids

Zhao Luo ^{1,*} , Zhendong Zhu ¹, Zhiyuan Zhang ¹, Jinghui Qin ¹, Hao Wang ¹, Zeyong Gao ¹ and Zhichao Yang ²

¹ Faculty of Electric Power Engineering, Kunming University of Science and Technology, Kunming 650500, China; zhuzhendong@stu.kust.edu.cn (Z.Z.); kgzhangzhiyuan@stu.kust.edu.cn (Z.Z.); qinjinghui@stu.kust.edu.cn (J.Q.); wanghao2@stu.kust.edu.cn (H.W.); gaozeyong@stu.kust.edu.cn (Z.G.)

² School of Electrical Engineering, Southeast University, Nanjing 210096, China; seuyangzhichao@seu.edu.cn

* Correspondence: waiting.1986@live.com

Received: 7 November 2019; Accepted: 12 December 2019; Published: 16 December 2019



Abstract: In order to reduce the impact of the randomness and volatility of renewable energy on the economic operation of AC/DC hybrid microgrids, a multi-time-scale rolling optimization strategy is proposed for the grid-connected AC/DC hybrid microgrids. It considers the source-load uncertainty declined with time scale reduction, and the scheduling cooperation problem of different units on different time scales. In this paper, we propose a three-time-scale optimal strategy of the day-ahead, intraday and real-time dispatching stage and a two-level rolling optimal strategy of the intraday and real-time stage, aiming at minimizing the operating cost. We added the power penalty cost in the rolling optimization model to limit the energy state of the energy storage system in the constraint, and improve the power correction and tracking effect of the rolling optimization. A typical-structure AC/DC hybrid microgrid is analyzed in this paper and the simulation results are shown to demonstrate the feasibility and effectiveness of the proposed multi-time-scale rolling optimal dispatch.

Keywords: microgrids; AC/DC hybrid; multi-time-scale; rolling optimization; energy management

1. Introduction

With the rapid increase of distributed energy supply in the power grid, more and more attention has been paid to the energy management of different types of distributed energy [1]. As an effective form of distributed generation access to the power grid, microgrids have been widely used in the electric power industry, among which AC microgrids have been a priority [2]. In recent years, DC-type distributed power supply and load have gained more attention in practical production because of the advantages of high efficiency and low loss [3]. AC/DC hybrid microgrid structure has become an important mode for DC distributed power supply and load access [4]. These forms of energy generation often have quite strong randomness, volatility and intermittency, so high-precision load forecasting algorithms are needed to support this AC/DC hybrid microgrid structure [5].

The AC/DC hybrid microgrids connect the distributed generator and load to AC and DC networks, respectively. Their optimal dispatching is more complex than AC microgrids. Relevant research has been carried out domestically and abroad. In [6], a decentralized power control method for grid-connected and isolated AC/DC hybrid microgrids was proposed, which adopts a different power exchange strategy for different operation conditions. The optimal dispatch of grid-connected AC/DC hybrid microgrids by combining a demand side response and energy storage operation was proposed in [7], and can effectively smooth tie-line power. The demand side management, which reduces the operation cost of microgrids, was added to the economic operation of AC/DC hybrid microgrids for peak cutting and valley filling in [8]. In [9], the operation mode of using a fixed strategy to formulate a

bidirectional converter adopted double-level optimal control to regulate the energy storage power in order to deal with the uncertainty of distributed generation and load. For the stochasticity of source-load, a two-level optimal scheduling model for planned power adjustment was proposed in [10], which also considers the access of electric vehicles. The above research only focuses on the optimal scheduling of the source-load power prediction data of a specific time scale of AC/DC hybrid microgrids. The deviation between the optimal results and actual scheduling is large. As the power prediction error of source-load decreases with the time scale shortening, the power prediction data in the near future should be used to optimize the dispatch of microgrids.

Considering the multi-time scale characteristics of the prediction data and the time-coupling relationship [11], the multi-time scale rolling optimization method has been applied to the economic dispatch of AC microgrids to deal with the source-load uncertainty problem [12]. A rolling optimization model for microgrid economic dispatch has been proposed [13], but it does not consider the relationship of multiple time scales. In [14], the energy management of an isolated AC microgrid is carried out from a two-time-scale including a day-ahead and intraday scale, and the rolling optimization of intraday only considers the state of charge (SOC) of tracking energy storage. In [15], an intraday dispatching is subdivided into a three-time-scale, and the rolling optimization results are closer to the superior optimization, but the response ability is reduced with the goal of minimizing the adjustment cost. A rolling optimization correction method based on model predictive control, which improves the effect of power correction to a certain extent, was proposed in [16]. However, its response characteristics did not improve much. The grid-connected AC/DC hybrid microgrids have many uncertainties of regional source-load, which greatly reduces the application effect of traditional rolling optimization. Existing rolling optimization studies have not considered the constraints of the initial and final states of energy storage in each rolling cycle, but there is a correlation between the initial and final states of energy storage in multiple time scales. In addition, the final states of energy storage in the last scheduling cycle in rolling optimization will be regarded as the initial states of energy storage in the next scheduling cycle. Without considering the initial and final states of energy storage, it is impossible to guarantee energy storage later. The cyclic regulation capability of continuous scheduling is not conducive to the economic operation of microgrids.

This paper synthesizes the multi-time scale characteristics of energy supply units in grid-connected AC/DC hybrid microgrids, and establishes a rolling optimal scheduling model with the three time scales of “day-ahead”, “intraday” and “real-time”. The operating cost is considered in the objective function of each time-scale model, and the power correction penalty cost of energy storage, two-way converter and grid-connected tie-line are added into the objective function of intra-day and real-time rolling optimization. In order to ensure the cyclic adjustment ability of the energy storage, the starting and ending energy state of the energy storage is defined in the constraint conditions. The validity and accuracy of the proposed model are verified by an example analysis. Compared with the traditional rolling optimization, the power correction and tracking effects are both improved.

2. Microgrid Structure and Operation Characteristics

AC/DC hybrid microgrids are divided into the AC side and the DC side. Both sides are connected with distributed power supply and energy storage devices, such as photovoltaic and wind turbine. The grid-connected AC/DC hybrid microgrids, whose typical structure is shown in Figure 1, are the focus in this paper.

As shown in Figure 1, the alternating current (AC) side of the microgrids is connected to wind turbine (WT) and AC load, while the direct current (DC) side is connected to photovoltaic (PV), energy storage and DC load. AC and DC buses are connected by bi-directional commutation devices, and the AC side of the microgrids is connected to the large grid to realize grid connection. During the operation of microgrids, AC load is mainly supplied by wind power, while DC load is supplied by photovoltaic energy. The energy storage system is used to suppress load fluctuation, peak cutting and valley filling. The bi-directional converter helps the AC and DC power flow in two directions, and

coordinates the operation of each region. In addition, when power gain or loss occurs in microgrids, power interaction can be carried out with microgrids.

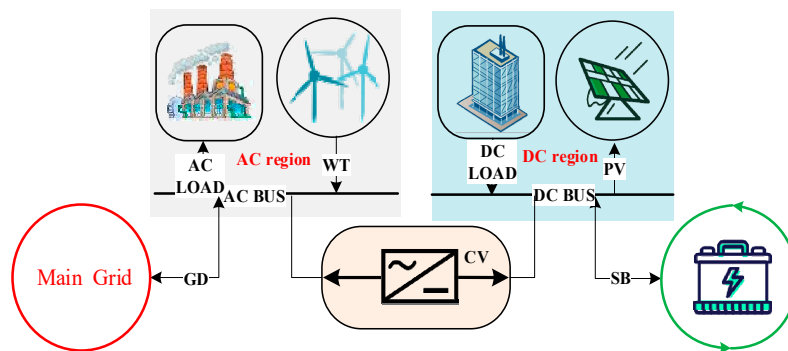


Figure 1. Structure of the grid-connected AC/DC hybrid microgrids.

The main operation characteristics of grid-connected AC/DC hybrid microgrids are as follows: (1). Distributed power supply on the AC side and the DC side should be given priority to supply power to each side respectively to meet the load demand in each region. (2). Power interaction between the AC side and the DC side through bidirectional converters can complement each other. (3). Energy storage can suppress power fluctuation on the AC side or the DC side. For the DC side, the storage system can charge and discharge directly, while for the AC side, the bi-directional converter affects the operation of energy storage. (4). There is a direct power interaction between the AC side and the main grid, but the interaction between the DC side and the main grid is also related to the bi-directional converter. In the traditional grid-connected AC microgrids, all power sources and loads are directly connected with AC buses. Their structure and operation mode are relatively simple. In the grid-connected AC/DC hybrid microgrids, AC and DC are separated. It is necessary to coordinate the DC side, AC side, large grid, and energy storage system all together to reach the power balance.

3. Multi-time Scale Rolling Optimization Architecture

In grid-connected AC/DC hybrid microgrids, the power prediction errors in different time scales will self-balance in the AC/DC region and reach commutation balance between regions. In addition, the residual power fluctuation will be balanced by the energy storage and the grid-connected tie-line. The rolling optimization reduces the error with the superior optimization result based on the above-mentioned balanced power fluctuation. There are many source-load cells in AC/DC hybrid microgrids, and the uncertainty of which calls for new requirements for system scheduling. In order to effectively manage the energy in grid-connected AC/DC hybrid microgrids and reduce the impact of uncertainty, this paper established a multi-time-scale rolling optimization model, which includes a three-time-scale optimal strategy and a two-level rolling optimization. The optimization process is shown in Figure 2.

(1) Day-ahead dispatching: Day-ahead dispatching uses 1 h as the time scale to forecast the wind and solar power load of 24 h in the coming day. According to the day-ahead forecast data and electricity price information, under the constraints of system and equipment operation, the next-day hourly operation power of each distributed power source, energy storage system, bidirectional converter, and tie-line is optimized with the objective of minimizing the operation cost of the microgrids. In addition, the day-ahead dispatching plan is formulated and delivered in advance. The optimization is executed once a day before the scheduling, and the results of optimization can be used as a reference for intraday dispatching.

(2) Intraday dispatching: Intraday dispatching uses 15 min as the time scale to predict the power of the next one hour. In order to reduce the impact of day-ahead prediction errors, the operation power of each subunit of the microgrids in the next 1 h and 15 min is optimized with the objective of

minimizing the system operation cost and equipment operation power, based on the predicted data of intraday and the optimization results of the day-ahead dispatch. The original operation plan is modified only by the optimization results in the next 15 min. Intraday dispatching is performed every 15 min, and the revised operation plan is used as a reference for real-time scheduling.

(3) Real-time dispatching: Real-time dispatching uses 5 min as the time scale to predict the power of the next 15 min. In order to reduce the impact of intraday prediction errors, real-time forecasting data and the optimization results of intra-day scheduling are needed for forecasting. With the goal of minimizing the system operating cost and equipment operating power correction, the operating power of each sub-unit of the microgrid will be rolling optimized every 5 min within the next 15 min, and only the scheduling plan for the next 5 min is revised.

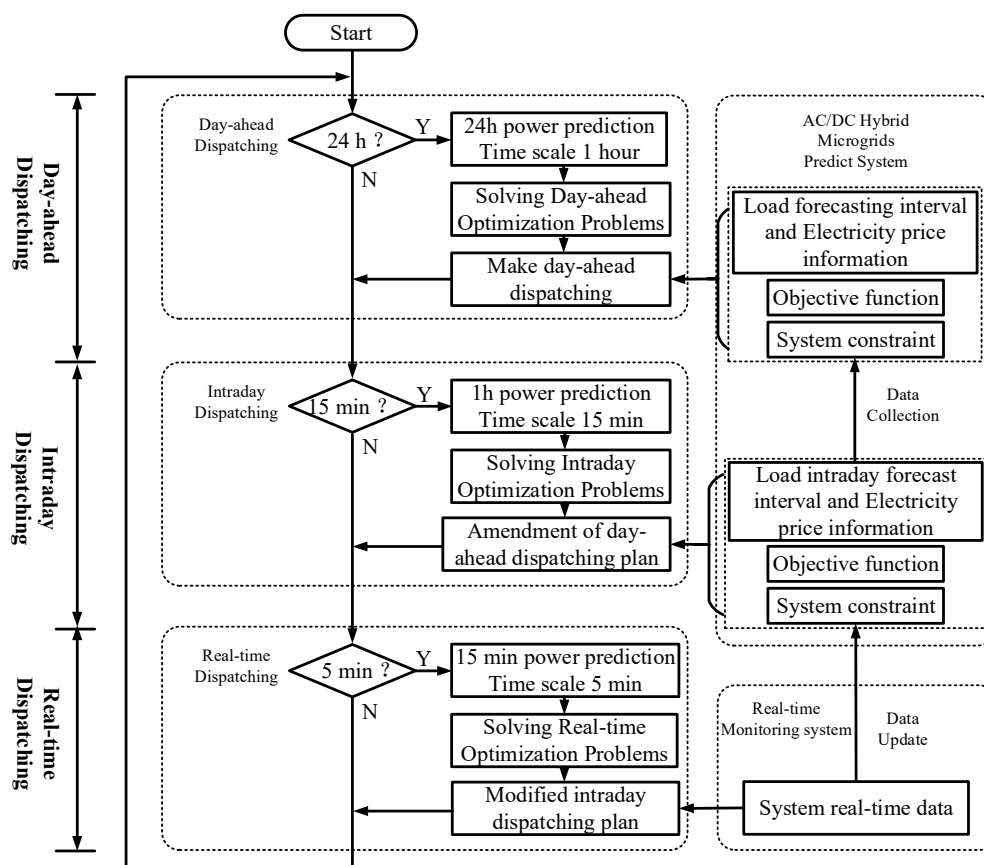


Figure 2. Flow chart for multi-time-scale rolling optimization.

4. Optimal Scheduling Model

The multi-time scale rolling optimal scheduling of grid-connected AC/DC hybrid microgrids includes three parts: day-ahead, intraday, and real-time dispatching. The detailed scheduling model described in this paper is as follows.

4.1. Day-Ahead Dispatching

The day-ahead dispatching optimization model for grid-connected AC/DC hybrid microgrids is established with the objective of minimizing the operation cost of microgrids. Dh represents day-ahead dispatching, and the objective function of the model is C^{Dh} .

$$\begin{cases} \min C^{\text{Dh}} = \sum_{i=1}^3 F_i \\ F1 = \sum_{t=1}^{N_t} \left[m_{\text{WT}} P_{\text{WT},t}^{\text{Dh}} + m_{\text{PV}} P_{\text{PV},t}^{\text{Dh}} + m_{\text{CV}} \left| P_{\text{CV},t}^{\text{Dh}} \right| \right] \Delta t \\ F2 = m_{\text{SB}} \sum_{t=1}^{N_t} \left| P_{\text{SB},t}^{\text{Dh}} \right| \Delta t \\ F3 = \sum_{t=1}^{N_t} m_{\text{GD},t} P_{\text{GD},t}^{\text{Dh}} \Delta t \end{cases} \quad (1)$$

where $F1$ is the total cost of equipment maintenance, $F2$ is the cost of energy storage, $F3$ is the cost of electricity purchase and sale, N_t is the total number of time periods in a scheduling cycle, m_{WT} , m_{PV} and m_{CV} are the maintenance cost coefficients of wind power, photovoltaic and bidirectional converter, respectively, m_{SB} is the cost coefficient of charge and discharge loss per unit of energy storage, which can be converted according to the investment cost of energy storage and the charge and discharge capacity of its life cycle, $m_{\text{GD},t}$ is the price of t period, and the price of purchasing and selling electricity is positive, and $P_{\text{WT},t}^{\text{Dh}}$, $P_{\text{PV},t}^{\text{Dh}}$, $P_{\text{CV},t}^{\text{Dh}}$, $P_{\text{SB},t}^{\text{Dh}}$ and $P_{\text{GD},t}^{\text{Dh}}$ represent the operation power of wind power generation, photovoltaic power generation, bidirectional converter, energy storage and contact line in t period, respectively. When the converter power flows from the DC side to the AC side, the $P_{\text{CV},t}^{\text{Dh}}$ is positive and vice versa. The size of $P_{\text{CV},t}^{\text{Dh}}$ represents the input power, $P_{\text{SB},t}^{\text{Dh}}$ represents charging, negative represents discharging, and $P_{\text{GD},t}^{\text{Dh}}$ represents purchasing power from the grid, and negative represents selling power to the grid.

The day-ahead dispatching of microgrids needs to satisfy the operational constraints of system and equipment. The main constraints in this paper are shown below:

(1) System Power Balance Constraints

(a) Total power balance constraints

$$P_{\text{WT},t}^{\text{Dh}} + P_{\text{PV},t}^{\text{Dh}} + P_{\text{GD},t}^{\text{Dh}} = P_{\text{LA},t}^{\text{Dh}} + P_{\text{LD},t}^{\text{Dh}} + (1 - \eta_{\text{CV}}) \left| P_{\text{CV},t}^{\text{Dh}} \right| + P_{\text{SB},t}^{\text{Dh}} \quad (2)$$

where $P_{\text{LA},t}^{\text{Dh}}$ is the AC side load in t period, $P_{\text{LD},t}^{\text{Dh}}$ is the DC side load in t period, and η_{CV} is the commutation efficiency of the converter.

(b) DC power balance constraints

$$\begin{cases} \Delta P_{\text{DC},t}^{\text{Dh}} = P_{\text{PV},t}^{\text{Dh}} - P_{\text{LD},t}^{\text{Dh}} \\ P_{\text{CV}',t}^{\text{Dh}} = \Delta P_{\text{DC},t}^{\text{Dh}} - P_{\text{SB},t}^{\text{Dh}} \\ P_{\text{CV},t}^{\text{Dh}} = \begin{cases} P_{\text{CV}',t}^{\text{Dh}} & P_{\text{CV}',t}^{\text{Dh}} \geq 0 \\ P_{\text{CV}',t}^{\text{Dh}} / \eta_{\text{CV}} & P_{\text{CV}',t}^{\text{Dh}} < 0 \end{cases} \end{cases} \quad (3)$$

where $\Delta P_{\text{DC},t}^{\text{Dh}}$ is the net power of the DC side. When the $P_{\text{CV}',t}^{\text{Dh}}$ is positive, the converting power flows from the DC side to the AC side. Conversely, the converting power flows from the AC side to the DC side.

(c) AC side power balance constraints

$$\begin{cases} \Delta P_{\text{AC},t}^{\text{Dh}} = P_{\text{WT},t}^{\text{Dh}} - P_{\text{LA},t}^{\text{Dh}} \\ P_{\text{GD},t}^{\text{Dh}} = \begin{cases} -\Delta P_{\text{AC},t}^{\text{Dh}} - P_{\text{CV},t}^{\text{Dh}} \eta_{\text{CV}} & P_{\text{CV},t}^{\text{Dh}} \geq 0 \\ -P_{\text{AC},t}^{\text{Dh}} - P_{\text{CV},t}^{\text{Dh}} & P_{\text{CV},t}^{\text{Dh}} < 0 \end{cases} \end{cases} \quad (4)$$

where $\Delta P_{\text{AC},t}^{\text{Dh}}$ is AC side net power.

(2) Power constraints of wind and solar power generation

$$\begin{cases} 0 \leq P_{WT,t}^{Dh} \leq P_{WTmax,t}^{Dh} \\ 0 \leq P_{PV,t}^{Dh} \leq P_{PVmax,t}^{Dh} \end{cases} \quad (5)$$

where $P_{WTmax,t}^{Dh}$ is the maximum output power of the fan in t period, and $P_{PVmax,t}^{Dh}$ is the maximum output power of photovoltaic in t period.

(3) Energy storage system constraints

(a) Energy storage constraints

$$\begin{cases} SOC_{min}^{Dh} \leq \frac{S_t^{Dh}}{E_C} \leq SOC_{max}^{Dh} \\ S_t^{Dh} = S_{t-1}^{Dh} + P_{SB,t}^{Dh} \Delta t \eta_C \\ S_t^{Dh} = S_{t-1}^{Dh} + P_{SB,t}^{Dh} \Delta t / \eta_D \end{cases} \quad (6)$$

where SOC_{min}^{Dh} and SOC_{max}^{Dh} are the lower and upper limits of the state of charge for energy storage, S_t^{Dh} and S_{t-1}^{Dh} are the remaining power of the energy storage system in t and $t - 1$ period, E_C is the rated capacity of energy storage, and η_C and η_D are the charging and discharging efficiencies of the energy storage system, respectively.

(b) Maximum charge and discharge power constraints

$$\begin{cases} -P_{Dmax,t}^{Dh} \leq P_{SB,t}^{Dh} \leq P_{Cmax,t}^{Dh} \\ P_{Cmax,t}^{Dh} = \min \left\{ P_{ch-max}, \frac{E_C \cdot SOC_{max}^{Dh} - S_{t-1}^{Dh}}{\Delta t \cdot \eta_C} \right\} \\ P_{Dmax,t}^{Dh} = \min \left\{ P_{disch-max}, \frac{[S_{t-1}^{Dh} - E_C \cdot SOC_{min}^{Dh}] \cdot \eta_D}{\Delta t} \right\} \end{cases} \quad (7)$$

where $P_{Cmax,t}^{Dh}$ and $P_{Dmax,t}^{Dh}$ are the allowable maximum charging and discharging power values of energy storage t period, and P_{ch-max} and $P_{disch-max}$ are the maximum charging and discharging continuous power set by the energy storage system itself.

(c) Constraints of equal starting and ending states

In order to ensure the cyclic charging and discharging operation of energy storage, the starting and ending states of energy storage need to be balanced.

$$S_0^{Dh} = S_{Nt}^{Dh} \equiv \text{const} \quad (8)$$

(4) Interactive power constraint of tie-line

$$|P_{GD,t}^{Dh}| \leq P_{GDmax}, P_{GD,t}^{Dh} \leq 0 \quad (9)$$

where P_{GDmax} is the maximum reverse power of the microgrids, only considering the selling time.

4.2. Intraday Dispatching

The intraday dispatching needs to refer to the day-ahead dispatching plan, respond to the power fluctuation caused by the prediction error in time, and track the optimization results of the upper level. Traditional rolling optimization achieves power response and tracking by adding power correction limits in constraints. Aiming at grid-connected AC/DC hybrid microgrids, this paper proposes a method of energy storage and tie-line power response and tracking, that is, the penalty term of power correction is added to the objective function of its intraday. And the initial and final energy state of energy storage is limited in the constraints.

The aim of intraday dispatching is to minimize the operating cost of microgrids, while the intraday dispatching model aims to change the symbol superscript of the day-ahead dispatching model from Dh to lh. In addition, a penalty term for correcting the operating power of AC/DC microgrid devices is added to the objective function of the intraday dispatching model.

$$F4 = \lambda_1 |P_{GD,t}^{lh} - P_{GD,t}^{Dh}| + \lambda_2 |P_{CV,t}^{lh} - P_{CV,t}^{Dh}| + \lambda_3 |P_{SB,t}^{lh} - P_{SB,t}^{Dh}| \quad (10)$$

where $F4$ is the penalty target value for correcting the operating power of the day-ahead dispatching equipment, λ_1 , λ_2 and λ_3 are the penalty factors for the day dispatching, and $P_{CV,t}^{lh}$, $P_{GD,t}^{lh}$ and $P_{SB,t}^{lh}$ are the operating power of the bidirectional converter, tie-line, and storage energy in the day dispatching t period, respectively.

The intraday dispatching of microgrids also needs to satisfy the operational constraints of the system and equipment, but the initial and final state constraints of each optimized energy storage system change to:

$$\begin{cases} S_0^{lh} = S_{Nt}^{Rh} \\ S_{Nt}^{lh} = S_{Nt}^{Dh} \end{cases} \quad (11)$$

where S_{Nt}^{Rh} is the remaining energy stored at the end of the last real-time dispatching cycle, and S_{Nt}^{Dh} is the remaining energy storage capacity of Nt in the corresponding period of day-ahead dispatch.

4.3. Real-Time Dispatching

Real-time dispatching changes the bid Dh in the previous day-ahead dispatching into Rh. In the objective function, a penalty item for correcting the operating power of the equipment is added:

$$F5 = \chi_1 |P_{GD,t}^{Rh} - P_{GD,t}^{lh}| + \chi_2 |P_{CV,t}^{Rh} - P_{CV,t}^{lh}| + \chi_3 |P_{SB,t}^{Rh} - P_{SB,t}^{lh}| \quad (12)$$

where $F5$ is the penalty target value of real-time dispatching equipment operation power correction, χ_2 , and χ_3 are the penalty factors of real-time dispatching, and $P_{CV,t}^{Rh}$, $P_{GD,t}^{Rh}$ and $P_{SB,t}^{Rh}$ represent the operation power of bidirectional converter, tie-line and energy storage, respectively, in the k period of real-time dispatching.

The real-time dispatching of microgrids satisfies the operational constraints of the system and equipment, but the initial and final state constraints of the energy storage system change to:

$$\begin{cases} S_0^{Rh} = S_{Nt}^{Rh} \\ S_{Nt}^{Rh} = S_{Nt}^{lh} \end{cases} \quad (13)$$

where S_{Nt}^{Rh} is the remaining energy stored at the end of the last real-time dispatching cycle, and S_{Nt}^{lh} is the remaining energy stored by Nt in the corresponding period of intraday dispatching.

5. Case Study

5.1. Case Parameters

A practical AC/DC hybrid microgrids system is taken as an example to analyze the multi-time scale rolling optimization. The equipment configuration and the cost coefficients in the optimization model are shown in Table 1.

The remaining equipment technical parameters and electricity prices are as follows:

(1). SB: SOC range [0.5,0.95], maximum charging power is 30 kW, maximum discharge power is 45kW, initial SOC is 0.8. (2). CV: maximum permissible commutation power is 100 kW, commutation efficiency is 0.95. (3). GD: maximum permissible selling power of the tie-line between the microgrid and main grid is 100 kW. (4). Electricity price is 0.28 yuan/kW·h, electricity price is 0.39 yuan/ kW·h.

In this paper, the actual engineering data of typical days are selected. The power forecasting data of wind power generation and AC/DC load in multi-time scales are shown in Figure 3. The deviation between the intraday forecasting data and the day-ahead forecasting data is less than 10%, and the deviation between the real-time forecasting data and the day-ahead forecasting data is less than 5%. The multi-time scale rolling optimization model established in this paper is a mixed-integer linear programming problem (MILP). The optimization problem uses MATLAB/YALMIP to model the optimization problem, and solves the problem using the CPLEX solver.

Table 1. Equipment parameters and cost factors.

Equipment	Configuration Paramete	Cost Coefficient/(yuan/kW·h)
WT	250 kW	0.01
PV	150 kW	0.01
SB	300 kW·h	0.01
CV	100 kW	0.04

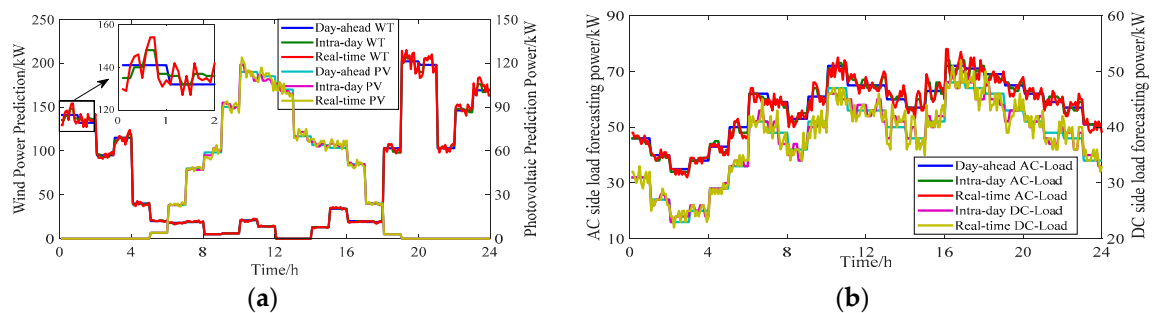


Figure 3. Predicted power of WT/PV and AC/DC loads. (a) Forecast wind power. (b) AC and DC load forecasting power.

5.2. Analysis of Optimization Results

In this paper, the optimal results of the day-ahead, intraday and real-time dispatching models are shown in Figures 4 and 5. Figure 4a,b are the optimal results of converter power and tie-line power in three-time-scale, respectively.

As shown in Figure 4, during the daytime, photovoltaic output meets the demand of the DC side load, while the wind power output is small, which cannot meet the demand of the AC side load. The net power of the DC side flows to the AC side, so the converter power is positive. However, the power of the wind-photovoltaic generation cannot meet the demand of all loads of the AC/DC hybrid microgrid. It needs to purchase power from the power grid, so the power of the tie-line is negative. During the night, the photovoltaic output is 0, but the wind power output is larger, so the net power of the AC side flows to the DC side, and the converter power is negative. Because of the small night load, the wind power generation can meet the demand of all loads, and the extra power can be sold to the main grid.

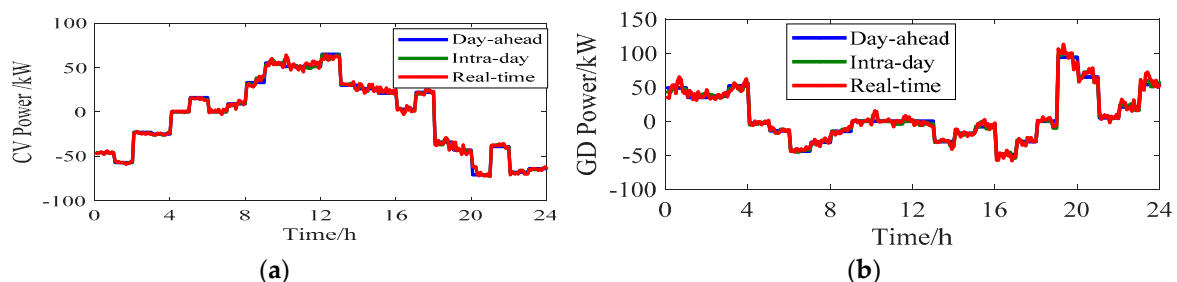


Figure 4. Optimal results of the tie-line power. (a) Converter power. (b) Power of tie-line.

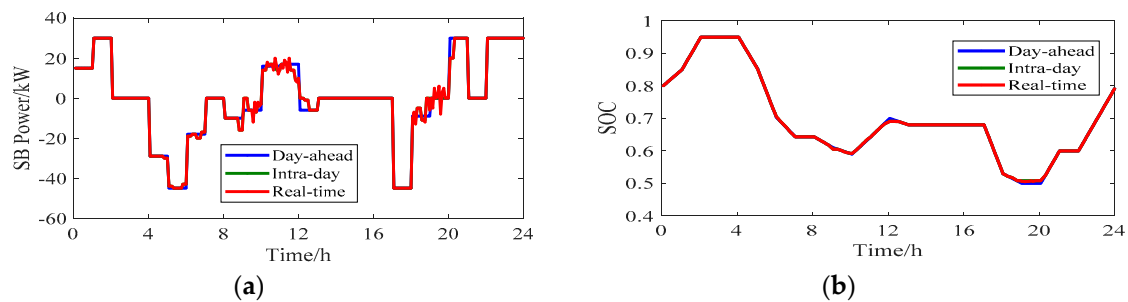


Figure 5. Optimal results of the energy storage parameters. (a) Energy storage power. (b) Energy storage SOC.

Figure 5a,b show the rolling optimization results of energy storage power and its charging state, respectively. As can be seen from Figure 5, the storage energy reaches the upper charge state limit after charging with more wind power at night. But in the morning, the wind power decreases and the photovoltaic power generation is insufficient, while load demand increases and energy storage discharges continuously, and the charging state reaches a low value. With the increase of photovoltaic output, the energy storage is charged when the photovoltaic output is large. At night, the photovoltaic output is reduced, and the wind power is insufficient. The energy storage is discharged at the peak of electricity consumption at night, and the state of charge reaches the lowest value in a day. The energy storage can effectively realize the function of peak and valley cutting. As shown in Figure 5b, the initial SOC of energy storage is 0.8. There are constraints of the same initial and final states in the optimization model, so the SOC is restored to 0.8 at the end of the scheduling cycle to ensure the sustainability of the storage scheduling.

There are errors in power prediction data in multi-time scales. For the grid-connected AC/DC hybrid microgrids, the power fluctuation caused by the prediction error is balanced by the energy storage system with power regulation and the grid-connected tie-line. The rolling optimization requires not only responding positively to power fluctuations caused by prediction errors but also tracking the results of superior optimization effectively and reducing power correction. As shown in Figures 4b and 5a, the optimization results of the tie-line and energy storage can track the day-ahead and intraday dispatching well. In order to quantify the response and tracking effect of rolling optimization, the optimization function values at three time scales and the superior optimization power correction results of energy storage and tie-line optimization are given in Table 2. The $\sum|\Delta P_{SB}|$ and the $\sum|\Delta P_{GD}|$ in the table are the sum of the power corrections of the energy storage and tie-line to the superior time scale at this time scale, respectively. The $\sum|P_{SB}|$ and $\sum|P_{GD}|$ are the sum of energy storage and tie-line operation power in this time scale, while the correction rate is the ratio of the sum of power correction and operation power.

Table 2. Objectives and power correction results.

Target Value	Day-Ahead	Intraday	Real-Time
$f/(\text{yuan})$	41.04	40.15	37.26
$\sum \Delta P_{SB} /(\text{kW})$	—	234	56
$\sum P_{SB} /(\text{kW})$	—	3894	3934
P_{SB} Correction rate/(%)	—	6.0	1.4
$\sum \Delta P_{GD} /(\text{kW})$	—	765	376
$\sum P_{GD} /(\text{kW})$	—	8031	8129
P_{GD} Correction rate/(%)	—	9.5	4.6

The analysis in Table 2 shows that with the decrease of time scale, the daily operating cost decreases from 41.04 yuan to 37.27 yuan. It can indicate that when the power prediction is revised with the previous time scale, the energy storage and tie-line can respond to the power fluctuation

and adjust the operating power in time, thus reducing the operating cost. Intraday and real-time corrections to energy storage power are 234 kW and 56 kW, respectively. The corrections to tie-line power are 765 kW and 376 kW, respectively. Because the prediction error decreases with time scale, the real-time correction is less than the intraday correction. In addition, the power range of the energy storage operation is smaller than that of the tie-line, so the power fluctuation of energy storage is smaller than that of the tie-line. The correction rates of energy storage and the tie-line are less than 10% in intraday rolling optimization, and the correction rates of real-time rolling optimization are less than 5%, indicating that energy storage and the tie-line effectively track the optimization results of superiors. The analysis above shows that the multi-time-scale rolling optimization model for grid-connected AC/DC hybrid microgrids established in this paper has good practicability.

5.3. Analysis of Operating Power Correction Constraints

Traditional rolling optimization often adds power correction limits to constraints. In this section, energy storage and tie-line operating power limits are added as constraints to the intraday and real-time dispatching model instead of Equations (10)–(13). The optimization results are compared with Section 4.2, as shown in Figure 6. It can be seen that the energy storage and tie-line can respond to power fluctuations in time for power regulation. However, the modified power of the energy storage and tie-line is obviously larger than that of Section 4.2, and the operation power of P_{SB} and P_{GD} fluctuates frequently. Table 3 gives the objective function values of rolling optimization in this section and the power correction values of energy storage and the tie-line.

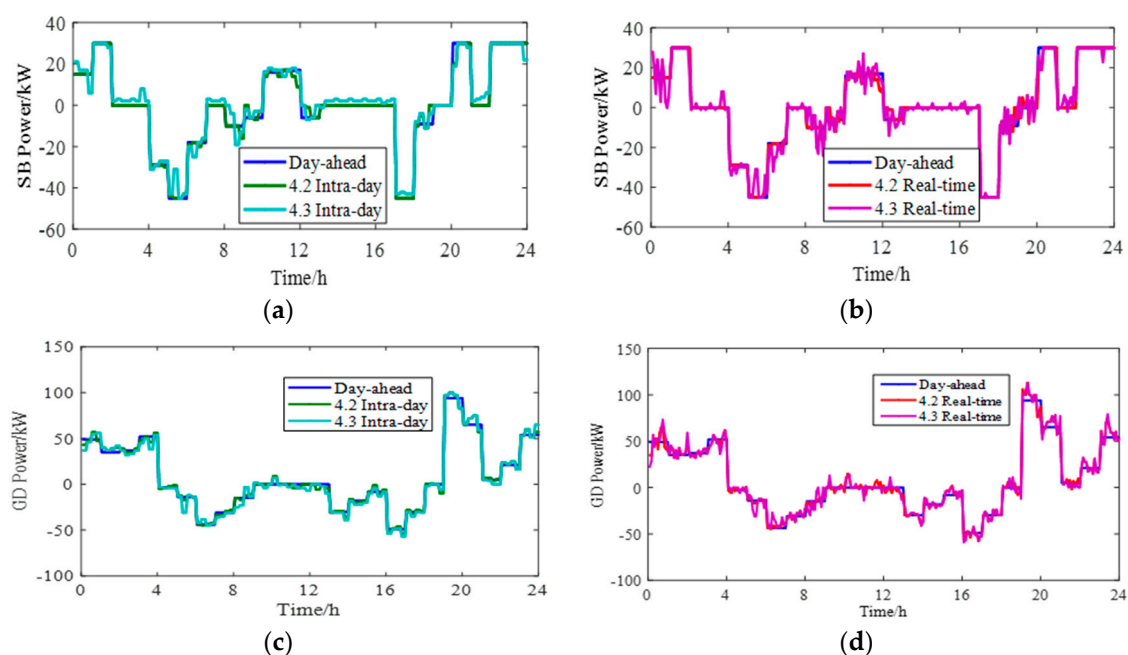


Figure 6. Optimal results under the restriction of power correction limits. (a) Energy storage power optimization results in a day. (b) Real-time optimization results of energy storage power. (c). Intra-day optimization of tie-line power. (d) Real-time optimization of tie-line power.

As shown in Table 3, the power adjustment of energy storage and the tie-line reduces the operation cost, but the objective function value is greater than that of Section 4.2. In terms of power correction values of energy storage and the tie-line, the data in Tables 2 and 3 show similar correction characteristics, i.e., real-time correction is less than intraday correction, and power fluctuation of energy storage is less than that of the tie-line. However, the correction amount in this section is larger. The function of the power correction limit constraint is similar to that of Equations (10)–(12), which allow the energy storage and tie-line to be responsive and tracked. Equations (11) and (13) increase

the constraints of the initial and final state of energy storage, and strengthen the connection between multiple time scales, which further improves the performance of rolling optimization. The analysis shows that the rolling optimization proposed in this paper has a better response and tracking effect than the traditional rolling optimization with power correction limit constraints.

Table 3. Objectives and power correction results under the restriction of power correction limits.

Target Value	Day-Ahead	Intraday	Real-Time
$f/(\text{yuan})$	41.47	40.56	37.52
$\sum \Delta P_{\text{SB}} /(\text{kW})$	—	729	163
$\sum P_{\text{SB}} /(\text{kW})$	—	4077	4093
P_{SB} Correction rate/(%)	—	17.9	4.0
$\sum \Delta P_{\text{GD}} /(\text{kW})$	—	1050	458
$\sum P_{\text{GD}} /(\text{kW})$	—	8214	8088
P_{GD} Correction rate/(%)	—	12.8	5.7

5.4. Constraints on the Initial and Final State of Energy Storage

The state constraints of Equations (11)–(13) make it necessary to adjust the power to reach the energy state at the end of the set period in the rolling optimization of energy storage, which increases the power correction of energy storage to a certain extent. In this section, the rolling optimization is carried out without considering the initial and final state constraints of energy storage. The optimization results are compared with those in Section 4.2, as shown in Figure 7. In Figure 7, the energy storage and tie-line still have better power response and tracking effect without the constraints of the initial and final states of energy storage. The correction power of energy storage in intraday and real-time optimization is less than that of Section 4.2, while the correction power of the tie-line is greater than that of Section 4.2. Table 4 presents the objective function values for rolling optimization and the power correction values for energy storage and the tie-line.

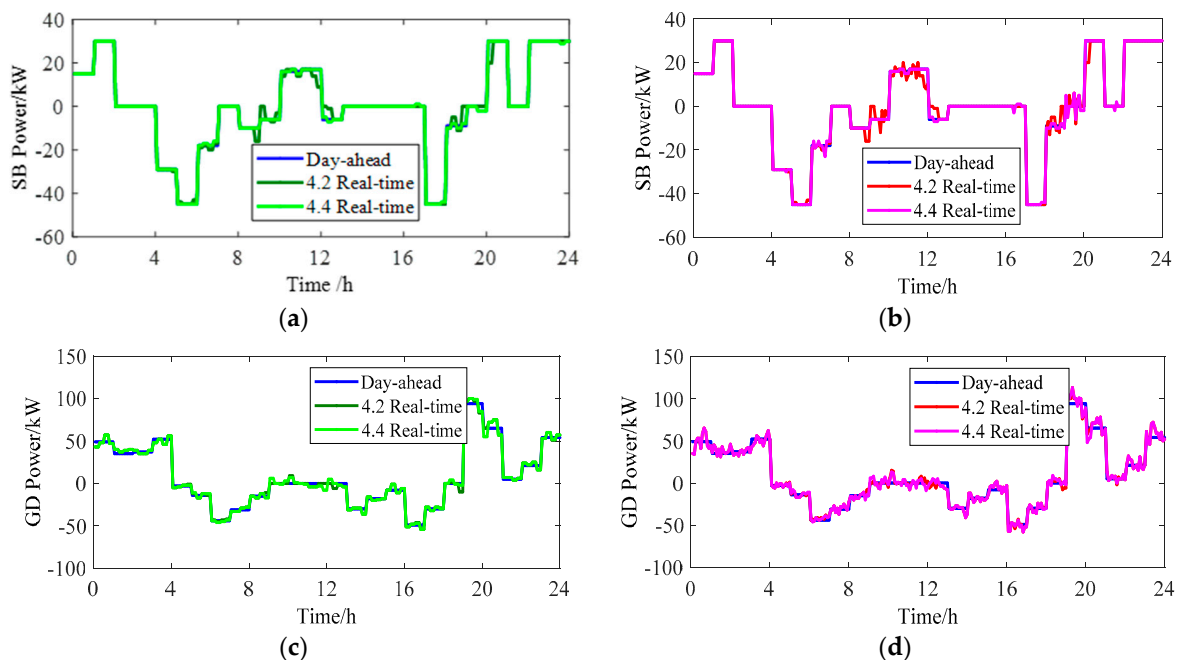


Figure 7. Optimal results without the SOC constraints. (a) Intraday optimization results of energy storage power. (b) Intraday optimization results of energy storage power. (c) Intraday optimization of tie-line power. (d) Real-time optimization of tie-line power.

Table 4. Objectives and power correction results without the SOC constraints.

Target Value	Day-Ahead	Intraday	Real-Time
$f/(\text{yuan})$	41.31	40.42	37.46
$\sum \Delta P_{\text{SB}} /(\text{kW})$	—	54	39
$\sum P_{\text{SB}} /(\text{kW})$	—	4032	4077
PSB Correction rate/(%)	—	1.3	1.0
$\sum \Delta P_{\text{GD}} /(\text{kW})$	—	831	389
$\sum P_{\text{GD}} /(\text{kW})$	—	8097	8166
P_{GD} Correction rate/(%)	—	10.3	4.8

As shown in Table 4, the operating cost, energy storage and power correction of the tie-line after the optimization in this section are all smaller than the results in Section 4.3, and the rolling optimization effect in this section is better than that of Section 4.3. Compared with the result of Section 4.2, the operating cost increasing indicates that the overall response effect of energy storage and the tie-line becomes worse. The power correction rate of energy storage decreases while the correction rate of the tie-line increases, indicating that the power fluctuation borne by the energy storage system decreases and the power fluctuation borne by the grid-connected tie-line increases. The power fluctuation originally assumed by energy storage was transferred to the tie-line. In summary, adding initial and final state constraints to energy storage in rolling optimization allows energy storage bear more power fluctuations and improve the response performance of rolling optimization.

6. Conclusions

The power prediction error will bring adverse effects on optimal dispatch of microgrids. Considering that the power prediction error decreases with the time scale decreasing, a multi-time scale rolling optimization strategy for grid-connected AC/DC hybrid microgrids is proposed in this paper, which aims at minimizing the total operation cost of the microgrids. The strategy includes the 1 h, 15 min and 5 min time scales optimization and a two-level rolling optimal strategy of intraday and real-time. A penalty cost of power correction is added to the objective function of the rolling optimization model. And the initial and final energy states of the energy storage system are limited in the constraints to ensure the cyclic regulation ability of the energy storage system and improve the power correction and tracking effect of the rolling optimization. This model is a mixed-integer linear programming problem, which can be solved efficiently by the CPLEX software.

The analysis of practical examples shows that the energy storage and tie-line can not only respond to the power fluctuation caused by the source-load power prediction errors on the DC and AC sides, but also track the operation plan of the upper level effectively. The state constraints at the initial and final energy states of energy storage are beneficial to ensure the cyclic operation of energy storage and improve the overall response performance of rolling optimization. However, it will reduce the ability of the energy storage tracking plan to run power. Compared with traditional rolling optimization, the proposed model is suitable for grid-connected AC/DC hybrid microgrids, and has a better optimization effect.

Author Contributions: Preparation of the manuscript has been performed by Z.L., Z.Z. (Zhendong Zhu), Z.Z. (Zhiyuan Zhang), J.Q., H.W., Z.G. and Z.Y.

Funding: This research was funded by the National Natural Science Foundation of China (No. 51907084), the Yunnan Provincial Talents Training Program (No. KKS201704027), and the Scientific Research Foundation of Yunnan Provincial Department of Education (No. 2018JS032). The authors would also like to gratefully thank the reviewer's suggestions and comments.

Conflicts of Interest: The authors declare no conflict of interest.

References

1. Liu, F.; Yang, X.; Shi, S. Economic operation of micro-grid based on sequence operation. *Trans. China Electrotech. Soc.* **2015**, *30*, 227–237.
2. Liu, N.; Li, Y.; Zhang, J. Hour-ahead optimization and real-time control method for micro-grid interconnection. *Trans. China Electrotech. Soc.* **2016**, *31*, 1–11.
3. Hosseinzadeh, M.; Salmasi, F.R. Power management of an isolated hybrid AC/DC micro-grid with fuzzy control of battery banks. *IET Renew. Power Gener.* **2015**, *9*, 484–493. [[CrossRef](#)]
4. Shaaban, M.F.; Eajal, A.A.; El-Saadany, E.F. Coordinated charging of plug-in hybrid electric vehicles in smart hybrid AC/DC distribution systems. *Renew. Energy* **2015**, *82*, 92–99. [[CrossRef](#)]
5. Wang, X.; Zhao, B.; Wu, H.; Zhang, X. Optimal sizing analysis of grid-connected hybrid AC-DC microgrids. *Autom. Electr. Power Syst.* **2016**, *40*, 55–62.
6. Li, J.H.; Wang, S.; Ye, L.; Fang, J.K. A coordinated dispatch method with pumped-storage and battery-storage for compensating the variation of wind power. *Prot. Control Mod. Power Syst.* **2018**, *3*, 21–34. [[CrossRef](#)]
7. Wang, D.; Ge, S.; Jia, H.; Wang, C.; Zhou, Y.; Lu, N.; Kong, X. A Demand Response and Battery Storage Coordination Algorithm for Providing Microgrids Tie-Line Smoothing Services. *IEEE Trans. Sustain. Energy* **2014**, *5*, 476–486. [[CrossRef](#)]
8. Kinhekar, N.; Padhy, N.P.; Li, F.; Gupta, H.O. Utility Oriented Demand Side Management Using Smart AC and Micro DC Grid Cooperative. *IEEE Trans. Power Syst.* **2015**, *31*, 1151–1160. [[CrossRef](#)]
9. Hosseinzadeh, M.; Salmasi, F.R. Robust Optimal Power Management System for a Hybrid AC/DC Micro-Grid. *IEEE Trans. Sustain. Energy* **2015**, *6*, 675–687. [[CrossRef](#)]
10. Eajal, A.A.; Shaaban, M.F.; Ponnambalam, K.; El-Saadany, E.F. Stochastic Centralized Dispatch Scheme for AC/DC Hybrid Smart Distribution Systems. *IEEE Trans. Sustain. Energy* **2016**, *7*, 1046–1059. [[CrossRef](#)]
11. Bao, Y.; Wang, B.; Li, Y.; Yang, S. Rolling Dispatch Model Considering Wind Penetration and Multi-scale Demand Response Resources. *Proc. Csee* **2016**, *36*, 4589–4599.
12. Silvente, J.; Kopanos, G.M.; Pistikopoulos, E.N.; Espuña, A. A rolling horizon optimization framework for the simultaneous energy supply and demand planning in microgrids. *Appl. Energy* **2015**, *155*, 485–501. [[CrossRef](#)]
13. Palma-Behnke, R.; Benavides, C.; Lanas, F.; Severino, B.; Reyes, L.; Llanos, J.; Sáez, D. A Microgrid Energy Management System Based on the Rolling Horizon Strategy. *IEEE Trans. Smart Grid* **2013**, *4*, 996–1006. [[CrossRef](#)]
14. Guo, S.; Yuan, Y.; Zhang, X. Energy Management Strategy of Isolated Microgrids Based on Multi-time Scale Coordinated Control. *Trans. China Electrotech. Soc.* **2014**, *29*, 122–129.
15. Dou, X.; Xu, M.; Dong, J.; Quan, X.J.; Wu, Z.J.; Sun, J. Multi-time Scale Based Improved Energy Management Model for Microgrids. *Autom. Electr. Power Syst.* **2016**, *40*, 48–55.
16. Hao, X.; Wei, P.; Li, K. Multi-time Scale Coordinated Optimal Dispatch of Microgrid Based on Model Predictive Control. *Autom. Electr. Power Syst.* **2016**, *40*, 7–14.



© 2019 by the authors. Licensee MDPI, Basel, Switzerland. This article is an open access article distributed under the terms and conditions of the Creative Commons Attribution (CC BY) license (<http://creativecommons.org/licenses/by/4.0/>).